Chromospheric Anemone Jets and Magnetic Reconnection in Partially Ionized Solar Atmosphere

K.A.P Singh,[1, a)] K. Shibata,[1, b)] N. Nishizuka,[2] and H. Isobe[3]

[1)]*Kwasan and Hida Observatories, Kyoto Univerisity, Yamashina, Kyoto 607-8471, Japan*

[2)]*Institute of Space and Astronautical Science (ISAS), Japan Aerospace Exploration Agency, 3-1-1, Yoshinodai, Chuo-ku, Sagamihara-shi, Kanagawa, Japan*

[3)]*Unit for Synergetic Studies for Space, Kyoto University, Yamashina, Kyoto 607-8471, Japan*

The Solar Optical Telescope (SOT) onboard Hinode with temporal resolution of less than 5 s and spatial resolution of 150 km has observed the lower solar atmosphere with an unprecedented detail. This has led to many important findings, one of them is the discovery of chromospheric anemone jets in the solar chromosphere. The chromospheric anemone jets are ubiquitous in solar chromosphere and statistical studies show that the typical length, life time and energy of the chromospheric anemone jets are much smaller than the coronal events (e.g. jets/flares/CMEs). Among various observational parameters, the apparent length and maximum velocity shows good correlation. The velocity of chromospheric anemone jets is comparable to the local Alfvén speed in the lower solar chromosphere. Since the discovery of chromospheric anemone jets by Hinode, several evidences of magnetic reconnection in chromospheric anemone jets have been found and these observations are summarized in this paper. These observations clearly suggest that reconnection occurs quite rapidly as well as intermittently in the solar chromosphere. In the solar corona ($\lambda_i > \delta_{SP}$), anomalous resistivity arises due to various collisionless processes. Previous MHD simulations show that reconnection becomes fast as well as strongly time-dependent due to anomalous resistivity. Such processes would not arise in the solar chromosphere which is fully collisional and partially-ionized. So, it is unclear how the rapid and strongly time- dependent reconnection would occur in the solar chromosphere. It is quite likely that the Hall and ambipolar diffusion are present in the solar chromosphere and they could play an important role in driving such rapid, strongly time-dependent reconnection in the solar chromosphere.

I. DISCOVERY OF CHROMOSPHERIC ANEMONE JET BY HINODE: AN INTRODUCTION

The heating of solar chromosphere and corona is a long lasting problem in solar physics. Space data gathered for last 20 years from various solar missions such as Yohkoh, SOHO, TRACE, and RHESSI have significantly improved our understanding of the dynamical processes in the solar corona. Recently, the high-resolution Solar Optical Telescope (SOT) onboard Hinode has discovered numerous Chromospheric Anemone Jets in the solar chromosphere[1]. A chromospheric anemone jet has a bright footpoint that has a cusp- or inverted Y-shaped structure (c.f. Fig. 1)[2]. Statistical study shows[2] that the chromospheric anemone jets have typical length $\sim$ 1.0 - 4.0 Mm, $\sim$ width 100 - 400 km, $\sim$ cusp size 700 - 2000 km, $\sim$ lifetime 100 - 500 s, and velocity $\sim$ 5 - 20 km s^{-1} . The Doppler velocity and occurrence height of the jet cannot be deduced from Ca IIH filter of SOT/Hinode

because it is a broadband type. Simultaneous observations with Hinode/SOT Ca IIH broadband filtergraph and the Ca IIK spectroheliograph on the Domeless Solar Telescope (DST) at Hida Observatory shows[3] that the jets are generated in the lower chromosphere since it cannot be seen in Ca IIK_3 . These jets are much smaller and occur much more frequently than the previously known jets, so called surges, and considered to be an indirect evidence of small-scale ubiquitous reconnection in the solar atmosphere as conjectured by Parker[1,4]. The characteristic shape of chromospheric anemone jet is similar to an X-ray anemone jet[5]. X-ray anemone jet is a coronal jet, ejected from an 'anemone-type' active region. On the basis of Yohkoh observations, an anemone shape is formed as a result of the magnetic reconnection between an emerging magnetic bipole and pre-existing uniform magnetic field (Fig. 2a). Once reconnection occurs between the emerging bipole and pre-existing uniform vertical field, the field lines with a polarity opposite to that of the ambient field become connected to the ambient polarity regions, forming a fan shape like that of a sea anemone[6]. This leads to an anemone shape at footpoint of the X-ray jet. Most of the footpoints of X-ray jets lie in the mixed polarity regions[5], providing an indirect evidence of magnetic

a)Electronic mail: singh@kwasan.kyoto-u.ac.jp

b)Also at Unit for Synergetic Studies for Space, Kyoto University, Yamashina, Kyoto 607-8471, Japan; Electronic mail: shibata@kwasan.kyoto-u.ac.jp
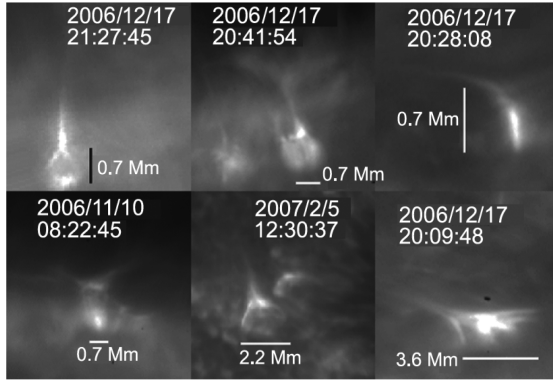
FIG. 1. Various chromospheric anemone jets observed by Solar Optical Telescope in Ca IIH. Note that the footpoint of jet has bright, inverse Y-shape or anemone shape structure[2].
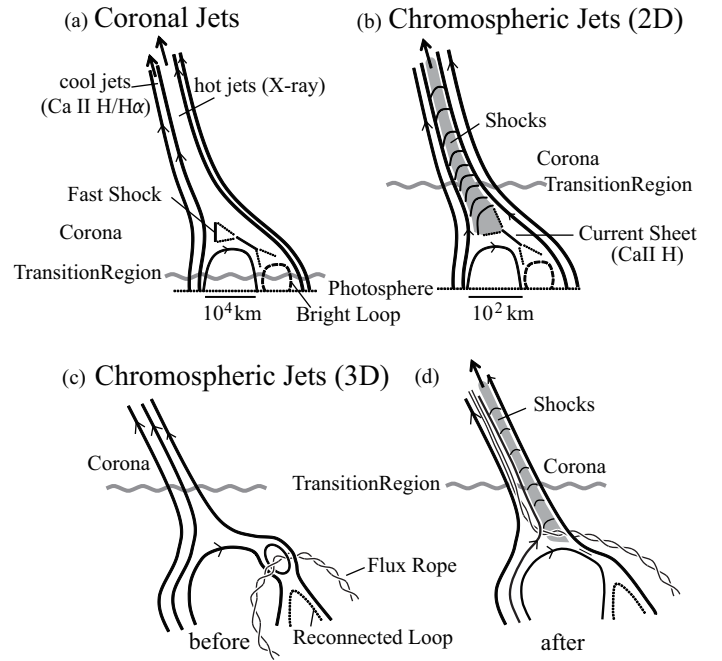

FIG. 2. Schematic diagram of Anemone Jets in (a) corona and (b) chromosphere in two-dimensions (2D). The three-dimensional (3D) evolution of chromospheric anemone jet (c) before and (d) after the reconnection is shown.

reconnection mechanism in the solar corona. The size of an anemone shape is determined by the size of an emerging bipole. If a small emerging bipole collides with the pre-existing field, an anemone shape with relatively smaller spatial scale will be formed as a result of magnetic reconnection. Since magnetic reconnection is a universal process that can occur on any spatial or temporal scales, it should occur not only in the corona but also in the photosphere and chromosphere which are fully collisional and partially ionized[7,8] (c.f. Table 2).

II. DYNAMICAL PROCESSES AND RECONNECTION FEATURES OBSERVED IN CHROMOSPHERIC ANEMONE JETS

The Ca IIH filtergram images from SOT/Hinode revealed that the chromosphere is very dynamic and filled with numerous jet-like structures such as spicules[9,10], penumbral microjets[11], and fibrils. Since the discovery of chromospheric anemone jets[1], several reconnection features have been observed in those jets and these features are summarized below.

a. *Apparent Velocity and Energy Estimates* The apparent velocity of chromospheric anemone jets is typically $\sim$ 5-20 km s^{-1}. The Alfvén speed in the low chromosphere is estimated to be $V_A \approx 10\ kms^{-1}(B/100\ G)\ (n/10^{15}cm^{-3})^{-0.5}$, so the apparent velocity of chromospheric anemone jet is close to the local Alfvén speed. Since the characteristic velocity of reconnection jet is close to the local Alfvén speed, the apparent velocity of jet is consistent with the reconnection model. An estimate of total stored energy (thermal+magnetic) at the footpoint suggests that a small-amount of energy, lying in the nanoflare regime (10^{23} - 10^{24} erg) is released due to reconnection[1] (c.f. Table 1). It is interesting to explore the relationship between ubiquitous jets and coronal heating, however, at present the number of these jets

is too small to explain the coronal heating[1].

b. *Reconnection Generated Alfvén Waves* Alfvén waves can be generated by magnetic reconnection[8,12–14]. In case of anemone jet, the Alfvén wave (more exactly kink wave) propagating along the jet should be observed because the jet is believed to be formed along the pre-existing magnetic field. Nishizuka et al. $(2008)^{15}$ observed a giant chromospheric anemone jet from SOT/Hinode and reported propagating Alfvén wave along the jet. The velocity of Alfvén wave $\sim$ 200 km s^{-1}, transverse velocity amplitude $\sim$ 5 - 15 km s^{-1} and wave period of $\sim$ 200 s is observed and this is in accordance with the simulation of chromospheric anemone jet which also shows generation and propagation of Alfvén waves along the cool jet.

c. *Multiple Plasma Ejections and Recurrent Nature* Observation of chromospheric anemone jets shows that they recur at the same location. Figure 3 shows downward ($\sim$ 35-50 km s^{-1}) as well as upward motion of a bright blob. These blobs are formed in one of the legs of inverse Y-shape footpoint. The upward moving blob gradually develops into jet. The light curve of the footpoint of jet shows many brightness enhancements (about 20 %-40 % of pre-brightening emission). Figure 4 shows a time evolution of jet and a bright, blob shape is visible at 12:19:19 UT. The height-time plot of jet shows many individual jets and a comparison of height-time plot with the light curve of footpoint shows that the footpoint brightening occurs before the formation of individual jets (Fig. 5). These observations provide a clear
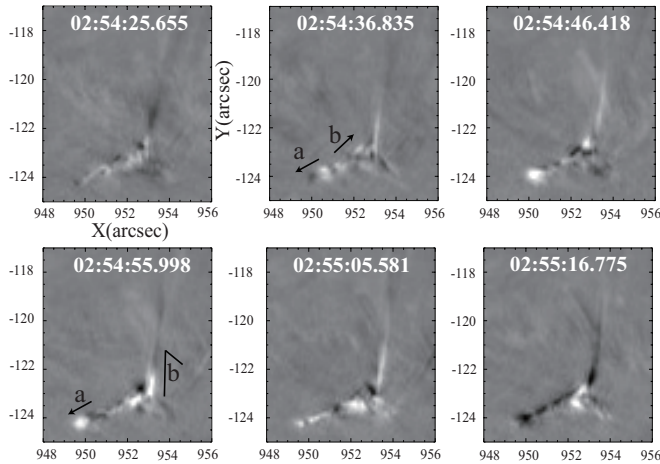
FIG. 3. Running difference image of chromospheric anemone jet observed on 14 January 2007 around 02:50 UT. A bright blob appeared on 02:54:36 UT which moved downwards 10 seconds later (a). At 02:54:56 UT, both bright blob and a jet is visible. The jet is formed by an upward moving bright blob (b) (visible during 02:54:46 UT) which gradually develops into jet. (Units on X- and Y-axes are in arcsecs and 1 arcsec = 725 km.)

evidence of plasmoid formation[16]. The temperature of reconnection heated plasma is given by $T_{rec} = T_0/\beta$, where T_0 is the background temperature and β is the plasma beta[17]. The plasma temperature increases at-most by a factor of 2 because plasma - β is near unity and the radiative time is short in the low chromosphere and photosphere. During the reconnection process the current sheet formed between the emerging bipole and pre-existing field get squeezed which results in the in-crease of density inside current sheet[15]. So the plasmoid appears bright in Ca IIH. However, the plasmoid soon after its formation collides with the pre-existing magnetic field and looses its blob like/or loop like shapes. This ex-plains why the ejecting plasma bundle has an elongated shape. The multiple plasma ejections from the footpoint of the jet shows that the reconnection occurs quite inter-mittently as well as in a strongly time-dependent manner in chromospheric anemone jets.

   d.   *Relationship with Hot Jets* The simulation in-volving magnetic reconnection driven by emerging flux shows that both hot and cool jets are produced simultaneously[15,18]. According to this model, X-ray and EUV jets are formed as hot jets and Ca jets or Hα surges are formed as cool jets (c.f. Fig 2a). The hot jets are pro-duced due to the magnetic reconnection (accelerated by enhanced gas pressure behind the fast shock) whereas the cool jets are produced due to the slingshot effect. The co-existence of hot and cool jet is confirmed sometimes by observations. It is important to mention that in or-der to produce both the hot and cool jets simultaneously, the reconnection point should lie in the transition region or in the upper chromosphere. Multiwavelength obser-
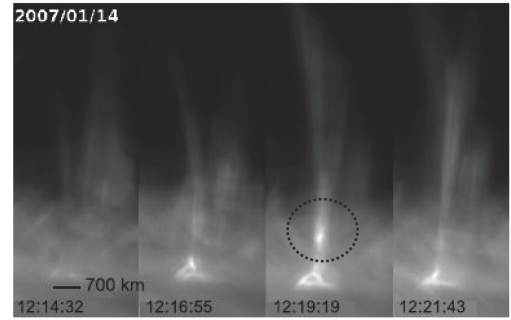

FIG. 4. Time evolution of a chromospheric anemone jet ob-served by SOT/Hinode on 14 January 2007. A bright blob and a bright loop is visible during 12:19:19 UT[1,2].
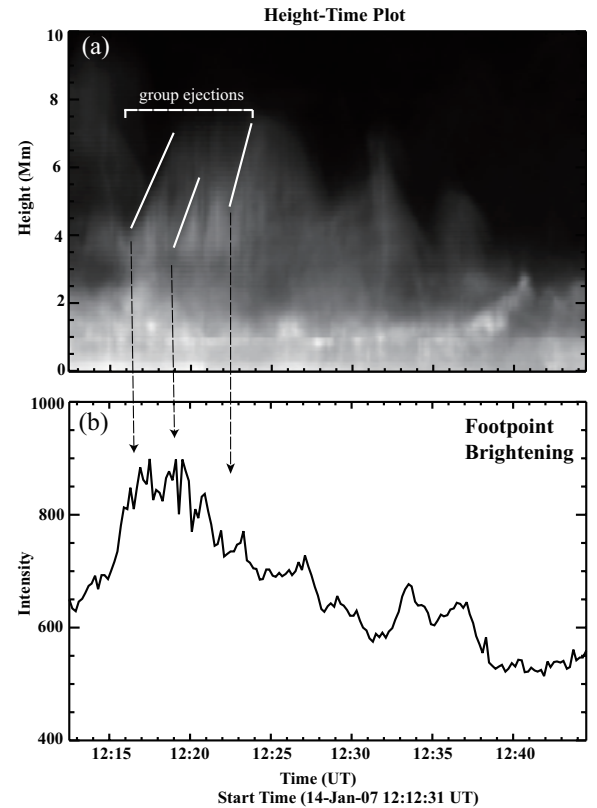

FIG. 5. The height-time plot of chromospheric anemone jet (a). The light curve of footpoint of chromospheric anemone jet is shown for comparison (b).

vation (Hinode/SOT, TRACE, XRT/Hinode) of jet pro-ducing region shows that an X-ray brightening/jet and a bright EUV jet appears at the same time and almost at the same place[15]. Once the bright, hot jets appear in X-ray and EUV, a cold plasma ejection is seen as a Ca jet and a dark EUV jet (jet-like feature that is dark in EUV because of absorption), and the time difference between the hot and cool plasma ejections is ~ 1 min - 2 min. This time scale can be compared with the ra-diative cooling time t_{rad} in the corona which is given
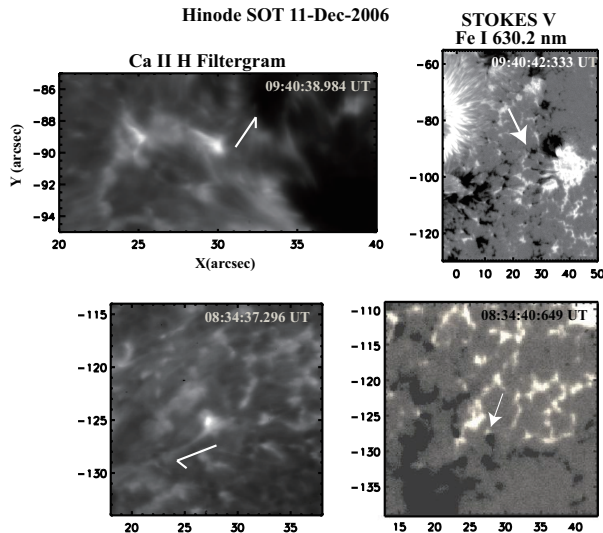
Hinode SOT 11-Dec-2006

Ca II H Filtergram

FIG. 6. Ca IIH image of chromospheric anemone jet taken with SOT/Hinode on 11 December 2006. Magnetograms (Fe I 630.2 nm narroband Stokes V image) during the onset of chromospheric anemone jet.

FIG. 7. Relationship between maximum length and velocity of Ca anemone jets (plus symbol +), which shows a good correlation[2]. Solid line indicates the distribution of jet length-jet velocity due to ballistic motion. The observed relationship between jet length-jet velocity is compared by the simulation result (shown by circle symbol o) of shock-acceleration model[20].

by $t_{rad} = 4000(\frac{n}{10^9 cm^{-3}})(\frac{T}{10^6 K})^2$ s. The coronal density $n=10^9$ cm^{-3} and $T=10^6$ K gives $t_{rad} \sim 1$ hour. So the observed time difference between the hot and cool jet can not be explained by the radiative cooling effect because it is much shorter than the cooling time. Since reconnection takes place between the coronal magnetic field consisting of hot and thin plasma, and the emerging flux in chromosphere consisting of cool and dense plasma, the reconnection is highly asymmteric. The asymmteric reconnection could account for the time difference because the low density part of the jet will move faster than the high density part or the faster jet will reach at higher altitudes earlier than the cool jet[15].

e. Relationship with Surrounding Magnetic Field The magnetic field observation from Hinode shows that footpoint of chromospheric anemone jet is located in the mixed-polarity regions, or near the boundary between opposite polarities, supporting the magnetic reconnection mechanism[1–3] (Fig. 6). The observation of Ca IIH brightenings near the disk center shows that they are associated with repeated, small-scale flux emergence event and the maximum brightness enhancements in Ca IIH occurs about 30 min after the positive flux starts to increase in the upper photosphere.[19]

f. Acceleration Mechanism of Jet The velocity of chromospheric anemone jet is $\sim$ 5 - 20 km s^{-1}, and the length is $\sim$ 1.0 -10.0 Mm. Among various observational parameters such as length, width, maximum velocity and lifetime, only apparent length and maximum velocity shows good correlation[2] (Fig. 7) . The height-time plot of three jets in Ca IIH shows typical height of the jet (c.f. Fig. 8a). If the jet undergoes ballistic motion, it cannot explain the observed height of the chromospheric anemone jet. This is because the max-
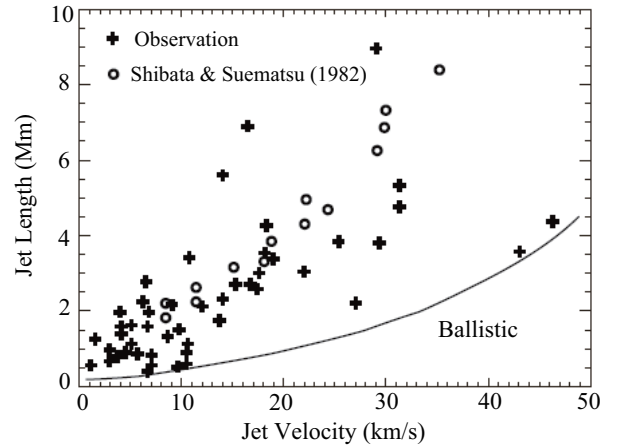
imum height the jet can attain due to ballistic motion is $\sim V_{jet}/(2g) \approx 200$ $km(V_{jet}/10$ $kms^{-1})^2$. Since the actual height of the jet is much larger than the scale height, there could be some additional mechanism that works on jet. One dimensional hydrodynamical simulation showed[20] that if the explosion occurs below the middle chromosphere, a slow mode wave ahead of the ejecta grows substantially into the shock which can accelerate the plasma and push it to 1 - 10 Mm height in the upper chromosphere. Spicules and small surges ejected from Ellerman bombs may be generated in this way[21]. The MHD simulation showed[22] that random horizontal photospheric motions of just 1 km s^{-1} generate Alfvén waves which propagate upwards and lift the transition region but it is found that the height of spicule is well determined by the slow mode excited by the nonlinear Alfvén wave (Fig. 8b).

g. Evidence of 3d Reconnection The 2D model of anemone jet explains the formation of single, collimated jet which is formed due to the reconnection between emerging bipole and pre-existing field[15]. In the 2D model, the footpoint has an anemone shape and the location of footpoint does not change during the jet activity (Fig. 2b). Hinode data shows that some of the chromospheric anemone jets have multi-threaded structure[16]. The multi-threaded structure of the jet can not be explained by the 2D model. Figure 9 shows some of the interesting examples. In some cases, the bright, plasma is ejected from the 'localized' footpoint in a direction that is oblique to the jet axis (top, Fig. 9). Such evolution of the jet can arise due to the sweeping-magnetic-twist mechanism[23]. In this model, a jet is formed due to the release of magnetic twist that is triggered due to the reconnection between a twisted loop and an open flux tube.
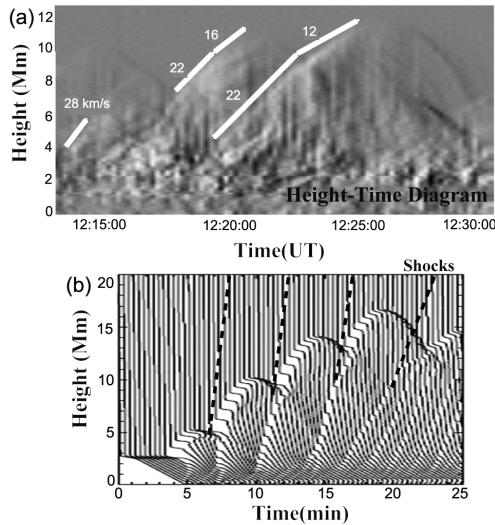
FIG. 8. Height-Time plot of Ca intensity along chromospheric anemone jets using running difference technique obtained from Ca II H broadband filter of SOT/Hinode. The numbers attached on curves denote velocity in units of km s^{-1}. Simulation result[22] of the time variation of density to explain the observed height of the jet[2].

During release of the magnetic twist, the jet exhibits a helical or whip-like motion that has been observed in some cases[24,25]. In some cases, the footpoint of jet has a loop and the jets are launched from one end of the loop to the other end in a systematic manner (middle, Fig. 9). Such behaviour can be explained by the successive reconnection along the neutral line[26,27]. However in some cases, the jets are formed in a sporadic manner and the location of footpoint/jet also changes (bottom, Fig. 9). These features indicate the role of 3D reconnection in chromospheric anemone jets (c.f. Fig. 2c,d).

III. MAGNETIC RECONNECTION IN PARTIALLY IONIZED PLASMA AND SOLAR CHROMOSPHERE

The time scale of reconnection in the solar chromosphere can be estimated from the lifetime of jets. A dimensionless reconnection rate can be obtained by normalizing the lifetime of chromospheric anemone jet by the local Alfvén time. The estimated dimensionless reconnection rates for various events shows that the reconnection in solar chromosphere occurs more rapidly than the solar corona[2] (c.f. Table 1). However, the reconnection rate in the solar chromosphere needs to be measured from the magnetic field data before any conclusion can be drawn. How such rapid reconnection could be realized in partially-ionized, fully collisional solar chromosphere? In case of the solar corona, anomalous resistivity arises because of various collisionless processes and it has been shown by MHD simulations that because of the anomalus resistivity the reconnection becomes fast as
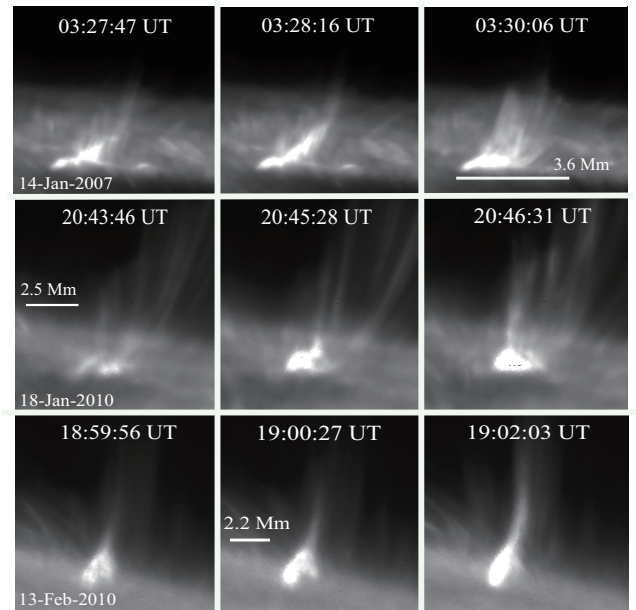

FIG. 9. Snapshots of three well resolved chromospheric anemone jets observed in Ca IIH by SOT/Hinode on 14 January 2007 (top), 18 January 2010 (middle) and 13 February 2010 (bottom). Notice that the footpoints of these jets show eruption and the jets have a multi-threaded structure.

well as strongly time- dependent[28–30]. Such collisionless processes are quite unlikely in the solar chromosphere.

The solar chromosphere is a partially ionized plasma and the collisions between electron, ion and neutral could play an important role in reconnection[31,32] (c.f. Table 2). The electron-ion and electron-neutral collisions develop an Ohmic resistivity[33]. On time-scales longer than ion-neutral collision time scales, the ambipolar diffusion between ion and neutrals arises and in addition to the ambipolar diffusion, Hall effect is also present at small scales. In a fully ionized plasma, Hall effect becomes important at scales close to ion-skin depth but in case of the collisional plasma such as solar photosphere/chromosphere, this length scale gets modified due to the ion-neutral collisions[33]. A comparison of various diffusivities in the solar atmosphere suggests that ambipolar diffusion is a dominant process in the solar chromosphere (Fig. 10).

To understand whether one-fluid collisional MHD applies to the solar chromosphere, it is important to compare the Hall- length scale with the resistive Sweet-Parker width (δ_{SP})[34]. The Sweet-Parker width in solar chromosphere is defined using electron-ion and electron-neutral collsions as $\delta_{SP} = \sqrt{\frac{L\eta}{V_A}}$, where the Ohmic magnetic difusivity (η) is given by

$$\eta = \lambda_e^2(\gamma_{ei} + \gamma_{en})$$

in cgs units, γ_{ei} and γ_{en} are the electron-ion and electron-neutral collision frequencies respectively. $\lambda_e(= \frac{c}{\omega_{pe}})$ is the electron skin-depth, $\omega_{pe}(= \sqrt{\frac{4\pi e^2 n_e}{m_e}})$ is the electron-

TABLE I. Comparison of Various "Flares "[a] observed in Solar Atmosphere.

"Flares "	Size (L)	Timescale (t)	Energy	B	n_e	V_A	t_A	t/t_A
	(10^3 km)	(s)	(erg)	(G)	cm^{-3}	km s^{-1}	(s)	
-	<0.2	<300	-	300	10^{16}	10	<20	10-20?
Nanoflares	0.2	200 - 100	10^{23} - 10^{26}	300	10^{16}	10	20	10-50
Microflares	5 - 40	60 - 600	10^{26} - 10^{29}	100	10^{10}	3000	5	12-120
Impulsive flares	10 - 100	60 - 3000	10^{29} - 10^{32}	100	10^{10}	3000	10	6-300
LDE flares	100 - 400	3×10^3 - 10^5	10^{30}-10^{32}	30	2×10^9	2000	90	30 - 10^3
Giant Arcades	300 - 1000	10^4 - 2×10^5	10^{29} - 10^{32}	10	3×10^8	1500	4000	25-500

[a] Types of mass ejection -in Nanoflares refers to chromospheric jets (anemone, penumbral), and even smaller events could be spicules; in Microflares refers to X-ray Jet/Hα; in Impulsive flares refers to X-ray plasmoid ejection/Hα filament eruption/spray; in LDE flares refers to X-ray plasmoid ejection/Hα filament eruption/CME; in Giant flares refers to X-ray plasmoid ejection/Hα filament eruption/CME.

TABLE II. Typical plasma parameters in partially ionized solar atmosphere [b].

height	Solar Photosphere		Solar Chromosphere	
	50 km	250 km	850 km	1000 km
T (K)	5790	4880	5650	6040
B (G)	1126	737	143	91
ρ_i	1.2×10^{-11}	9.4×10^{-14}	1.75×10^{-13}	1.7×10^{-13}
ρ_n	1.6×10^{-7}	3.9×10^{-8}	1.7×10^{-10}	3.6×10^{-11}
γ_{ei}	9.4×10^8	9×10^6	1.3×10^7	1.2×10^7
γ_{en}	4.5×10^9	1×10^9	4.6×10^6	1×10^6
γ_{in}	7.5×10^8	1.7×10^8	7.7×10^5	1.7×10^5
η	7.8×10^7	1×10^8	4.2×10^7	3.4×10^7
η_H	2.8×10^8	1.4×10^9	9×10^9	4.3×10^9
η_{amb}	1×10^7	2.7×10^9	1.2×10^{10}	2.3×10^{10}

[b] in CGS units. γ_{ei}, γ_{en}, γ_{in} are the electron-ion, electron-neutral and ion-neutral collision frequencies respectively. η is the Ohmic magnetic diffusivity arising due to electron-ion and electron-neutral collisions. η_H is the Hall magnetic diffusivity and η_{amb} is the ambipolar magnetic diffusivity.
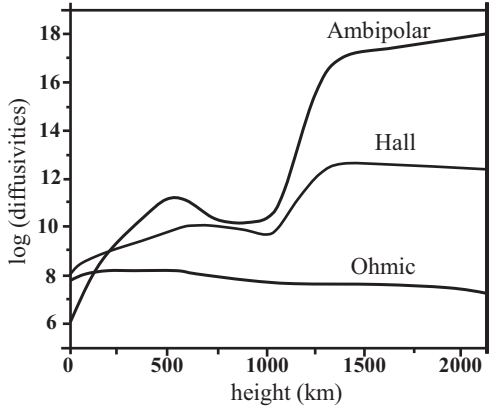

FIG. 10. Ambipolar (η_{amb}), Hall (η_H) and Ohmic (η) diffusivities as a function of height above the solar surface.

plasma frequency and V_A is the Alfvén speed. The electron mean free path (λ_{mfp}) in the chromosphere is typically ~ 50 cm. The Hall magnetic diffusivity is given by

$$\eta_H = \frac{cB}{4\pi e n_e}$$

in cgs units, where n_e is the electron density. Note that in case of the solar corona, the Sweet-Parker width is defined using Spitzer's resistivity ($\eta_{cor} = \lambda_e^2 \gamma_{ei}$). In a partially ionized plasma, the Hall- length scale is modified because of the ion-neutral collisions. We can define ratio ($\Re$) of Hall- length scale to Sweet Parker width as[16]

$$\Re = \sqrt{\frac{\rho_n}{\rho_i}} \frac{c}{\omega_{pi}} \sqrt{\frac{V_A}{\eta L}}$$

where $\omega_{pi} (= \sqrt{\frac{4\pi e^2 n_i}{m_i}})$ is the ion-plasma frequency for proton. The ion-skin depth is defined as $\lambda_i = \frac{c}{\omega_{pi}}$. Typical values of Sweet-Parker width is estimated assuming, $\eta = 10^7$ cm^2 s^{-1}, $L=10^8$ cm, $V_A=10^6$ cm/s, and $R_m = LV_A/\eta = 10^7$ that gives the Sweet-Parker width ($\delta_{SP} = LR_m^{-1/2}$) $\sim 10^5$ cm. The Hall-length scale ($= \sqrt{\frac{\rho_n}{\rho_i}} \lambda_i$) is $\sim 10^3$ cm, assuming $\frac{\rho_n}{\rho_i} = 10^3$ and $\lambda_i = 100$ cm. This suggests that the chromosphere is in collisional regime and one may think of the Sweet-Parker reconnection in the chromosphere. So, how a Sweet-Parker current sheet is involved in the fast reconnection process in the chromosphere. The ambipolar drift ($\vec{V} = \vec{V_i} - \vec{V_n}$) is given by $V = \eta_{amb}/\delta_{SP}$ where η_{amb} is the ambipolar

magnetic diffusivity given by

$$\eta_{amb} = \frac{V_{Ai}^2}{\gamma_{in}}$$

in cgs units, where γ_{in} is the ion-neutral collision frequency[33]. The ambipolar diffusivity (η_{amb}) is $\sim 10^{10}$ cm^2 s^{-1}. This gives an ambipolar drift of ~ 1 km s^{-1} just outside the resistive Sweet-Parker layer. Comparing the Sweet-Parker width arising due to the ambipolar diffusion $\delta_{amb} = \sqrt{\frac{L\eta_{amb}}{V_A}}$, with δ_{SP} gives $\delta_{amb}/\delta_{SP} = (\eta_{amb}/\eta)$ i.e. $\delta_{SP} < \delta_{amb}$. This suggests that ambipolar diffusion dominates just outside the resistive Sweet-Parker current sheet. A resistive Sweet-Parker current sheet in the presence of ambipolar diffusion would be unstable for tearing mode instability[35]. As a result of the tearing mode instability, multiple plasmoids will be formed and once such plasmoids are ejected, a time-dependent reconnection can occur[36]. The tearing mode time scale ($\tau_{tearing}$) for the most unstable wavelength is given by $\tau_{tearing} = (\tau_A \tau_d)^{0.5}$, where τ_A is the Alfvén time defined w.r.t total density and τ_d is the resistive diffusion time. Due to the ambipolar diffusion, the neutrals decouple on smaller scales from the plasma, so the characteristic Alfvén time is $\tau_{Ai} = \tau_A \sqrt{\frac{\rho_i}{\rho_n}}$. The tearing mode time scale for the most unstable wavelength due to the ambipolar diffusion ($\tau_{tearing,amb}$) can be estimated by $\tau_{tearing,amb} = (\tau_{Ai} \tau_d)^{0.5}$. This suggests that the tearing mode instability grows faster in the presence of ambipolar diffusion. Assuming $\delta_{SP} \simeq 10^6$ cm, $\eta \simeq 10^7$ cm^2 s^{-1}, $V_{Ai} \simeq 300$ km s^{-1} (Alfvén speed w.r.t ions), $\tau_{tearing,amb} \simeq 50$ s.

In conclusion, SOT/Hinode has shown several pieces of evidences of strongly, time-dependent magnetic reconnection in the solar chromosphere. Since the solar chromosphere is partially ionized, it is quite likely that the Hall effect and the ambipolar diffusion are present that could play an important role in driving such rapid, strongly time-dependent reconnection in the solar chromosphere.

[1] K. Shibata, T. Nakamura, T. Matsumoto, K. Otsuji, T.J. Okamoto, N. Nishizuka, T. Kawate, H. Watanabe, S. Nagata, S. Ueno, R. KItai, S. Nozawa, S. Tsuneta, Y. Suematsu, K. Ichimoto, T. Shimizu, Y. Katsukawa, T.D Tarbell, T.E. Berger, B.W. Lites, R.A. Shine, and A.M. Title, Science 318, 1591 (2007).

[2] N. Nishizuka, T. Nakamura, T. Kawate, K.A.P. Singh, and K. Shibata, Astrophys. J. 731, 43 (2011).

[3] S. Morita, K. Shibata, S. Ueno, K. Ichimoto, R. Kitai, and K.-I. Otsuji, Pub. Astron. Soc. of Japan 62, 901 (2010).

[4] E.N. Parker, Astrophys. J. 330, 474 (1988).

[5] M. Shimojo, K. Shibata, and K.L. Harvey, Sol. Phys. 178, 379 (1998).

[6] K. Shibata, N. Nitta, K.T. Strong, R. Matsumoto, T. Yokoyama, T. Hirayama, H. Hudson, and Y. Ogawara, Astrophys. J. 431, L51 (1994).

[7] Y.E. Litvinenko, Astrophys. J. 515, 435 (1999).

[8] T. Takeuchi and K. Shibata, Astrophys. Lett. 546, L73 (2001).

[9] Y. Suematsu, K. Ichimoto, Y. Katsukawa, T. Shimizu, T. Okamoto, S. Tsuneta, T. Tarbell, and R.A. Shine, Astron. Soc. of Pac. Conf. Series 397, 27 (2008).

[10] B. De Pontieu, S.W. McIntosh, M. Carlsson, V.H. Hansteen, T.D. Tarbell, P. Boerner, J. Martinez-Sykora, C.J. Shrijver, and A.M. Title, Science 331, 55 (2011).

[11] Y. Katsukawa, T.E. Berger, K. Ichimoto, B.W. Lites, S. Nagata, T. Shimizu, R.A. Shine, Y. Suematsu, T.D. Tarbell, A.M. Title, and S. Tsuneta, Science 331, 1594 (2007).

[12] T. Yokoyama and K. Shibata, Astrophys. Lett. 494, L113 (1998).

[13] N. Nishizuka and K. Shibata, Astron. Soc. of Pacific. Conf. Series 415, 188 (2009).

[14] H. Kigure, K. Takahashi, K. Shibata, T. Yokoyama, and S. Nozawa, Pub. Astron. Soc. of Japan 62, 993 (2010).

[15] N. Nishizuka, M. Shimizu, T. Nakamura, K.-I. Otsuji, T.J. Okamoto, Y. Katsukawa, and K. Shibata, Astrophys. Lett. 683, L83 (2008).

[16] K.A.P. Singh, H. Isobe, N. Nishizuka, K. Nishida, and K. Shibata, Astrophys. J. to be submiited (2011).

[17] T. Yokoyama and K. Shibata, Pub. Astron. Soc. of Japan 48, 353 (1996).

[18] T. Yokoyama and K. Shibata, Nature 375, 42 (1995).

[19] S.L. Guglielmino, F. Zuccarello, P. Romano, and L.R. Bellot Rubio, Astrophys. J. 688, L111 (2008).

[20] K. Shibata and Y. Suematsu, Sol. Phys. 78, 333 (1982).

[21] Y. Suematsu, K. Shibata, T. Neshikawa, and R. KItai, Sol. Phys. 75, 99 (1982).

[22] T. Saito, T. Kudoh, and K. Shibata, Astrophys. J. 554, 1151 (2001).

[23] K. Shibata and Y. Uchida, Sol. Phys. 103, 299 (1986).

[24] W. Liu, T.E. Berger, A.M. Title, and T.D. Tarbell, Astrophys. Lett. 707, L37 (2009).

[25] W. Liu, T.E. Berger, A.M. Title, T.D. Tarbell, and B.C. Low, Astrophys. J. 728, 103 (2011).

[26] H. Isobe, K. Shibata, and S. Machida, Geophys. Res. Lett. 29, 210000 (2002).

[27] T. Shimizu, Y. Katsukawa, M. Kubo, B.W. Lites, K. Ichimoto, Y. Suematsu, S. Tsuneta, S. Nagata, R.A. Shine, and T.D. Tarbell, Astrophys. Lett. 696, L66 (2009).

[28] M. Ugai and T. Tsuda, Phys. of Plasmas 17, 337 (1977).

[29] T. Yokoyama and K. Shibata, Astrophys. Lett. 436, L197 (1994).

[30] R.A. Truemann, Earth, Planets and Space 53, 453 (2001).

[31] E.G. Zweibel, Astrophys. J. 340, 550 (1989).

[32] E.T. Vishniac and A. Lazarian, Astrophys. J. 511, 193 (1999).

[33] K.A.P. Singh and V. Krishan, New Astron. 15, 119 (2010).

[34] M. Yamada, Y. Ren, H. Ji, B. Joshua, G. Stefan, R. Kulsrud and A. Kuritsyn, Phys. Plasmas. 13, 052119 (2006).

[35] H. Isobe and others, in prep (2011).

[36] K. Shibata and S. Tanuma, Earth, Planets, and Space 53, 473 (2001).